Optics and Lasers in Engineering 95 (2017) 1–7

Contents lists available at ScienceDirect

Optics and Lasers in Engineering

journal homepage: www.elsevier.com/locate/optlaseng

Anti-spoof touchless 3D fingerprint recognition system using single shot fringe projection and biospeckle analysis

Amit Chatterjee[a], Vimal Bhatia[a], Shashi Prakash[b,*]

[a] Signals and Software Group, Discipline of Electrical Engineering, Indian Institute of Technology, Indore 453446, India
[b] Photonics Laboratory, Department of Electronics & Instrumentation Engineering, Institute of Engineering & Technology, Devi Ahilya University, Khandwa Road, Indore 452001, India

ABSTRACT

Fingerprint is a unique, un-alterable and easily collected biometric of a human being. Although it is a 3D biological characteristic, traditional methods are designed to provide only a 2D image. This touch based mapping of 3D shape to 2D image losses information and leads to nonlinear distortions. Moreover, as only topographic details are captured, conventional systems are potentially vulnerable to spoofing materials (e.g. artificial fingers, dead fingers, false prints, etc.). In this work, we demonstrate an anti-spoof touchless 3D fingerprint detection system using a combination of single shot fringe projection and biospeckle analysis. For fingerprint detection using fringe projection, light from a low power LED source illuminates a finger through a sinusoidal grating. The fringe pattern modulated because of features on the fingertip is captured using a CCD camera. Fourier transform method based frequency filtering is used for the reconstruction of 3D fingerprint from the captured fringe pattern. In the next step, for spoof detection using biospeckle analysis a visuo-numeric algorithm based on modified structural function and non-normalized histogram is proposed. High activity biospeckle patterns are generated because of interaction of collimated laser light with internal fluid flow of the real finger sample. This activity reduces abruptly in case of layered fake prints, and is almost absent in dead or fake fingers. Furthermore, the proposed setup is fast, low-cost, involves non-mechanical scanning and is highly stable.

1. Introduction

A fingerprint is a mark or an impression made on a surface by friction ridges of a person's fingertip [1]. Fingerprints of human being are nearly unique, detailed, difficult to alter and durable for entire life. In forensic science, several physical and behavioral traits (e.g. DNA, iris, fingerprint, signature, face, etc.) are used for identifying and authenticating individuals. Among them, fingerprint is considered as most reliable due to its simplicity, easy and non-destructive collectability, etc. For many years, fingerprints have been used in different and versatile applications like in a criminal investigation, for identification and authentication in driving license, computer network login authentication, electronic data security, credit card, physical access control, cellular phone, etc. Hence, for detection and analysis of the fingerprint, wide ranges of techniques have been developed.

Traditional fingerprint recognition is mostly performed by 2D imaging methods like the ones based on ink, capacitance of finger constituents, ultrasound, thermal or an imaging device as a CCD or a CMOS camera. Among these approaches, the most popular method is the use of contact based devices. The contact based devices perform geometric difference between ridge and furrow patterns to extract the fingerprint information. In this approach, finger has to be placed on a hard or semi-hard surface, leading to inconsistency and distortions. In many applications where high precision as well as high security is required (like the government or financial institutions, army bases, defense and nuclear research labs, etc.), conventional scanners fail to provide the desired service due to a number of reasons. First, unavoidable distortions are generated because of factors such as inconsistent 3D to 2D mapping, non-uniformity in the finger pressure on the device, etc. Second, careful maintenance of the sensor or prism is required in order to avoid erroneous data. Third, other external factors like non-uniform illumination, the finger skin condition (dry or wet), and the residue of the previous fingerprints or the environmental perturbations may adversely affect performance of the device. Finally, “spoofing attacks”, wherein a false biometric is forged in order to gain spurious access are increasing day by day. Spoof attacks are gaining popularity because other forms of unauthorized data access require in-depth knowledge regarding the network and extensive hacking skills. Also, artificial

* Corresponding author.
E-mail address: sprakash_davv@rediffmail.com (S. Prakash).

http://dx.doi.org/10.1016/j.optlaseng.2017.03.007
Received 18 November 2016; Received in revised form 1 March 2017; Accepted 22 March 2017

dummies with embedded fingerprints can be prepared from household supplies, costing less than $10. Therefore, security provided by the conventional fingerprint scanners need to be strengthened by investing efforts into the development of newer techniques.

With the development of technology, touchless 3D biometry has been studied by a few researchers in recent years. The 3D biometry not only overcomes the drawbacks of conventional fingerprint scanner, but also provides robustness against fraud and clutter because it is extremely difficult to replicate a 3D finger with its ridge-valley pattern. Towards this, Parziale et al. [2] proposed a multi-camera device named "The Surround Imager™" for the acquisition of 3D rolled-equivalent fingerprints. The device contains an array of 16 LEDs and a cluster of 5 cameras arranged in a semicircle pointing to its center. As the finger is placed in the desired position, all the cameras capture images from different angles; 3D reconstruction is achieved by combining all the images using a complex and computationally expensive algorithm. Wang et al. [3] proposed a 3D non-contact method based on phase measuring profilometry which is simply an extension of classical interferometric technique. A number of phase shifted fringes are projected onto the surface of a finger by a DLP projector and the deformed pattern is captured by a CCD camera. Recently, Huang et al. [4] proposed an improved technique based on phase-shifted fringe projection to obtain profile of a fingerprint along with its color texture information. Here, four-step phase shifting is combined with optimum three-fringe number selection algorithm that independently evaluates absolute phase at each pixel position. However, these methods are prone to environmental noise and perturbations, especially during the period when the phase shifted images are captured [5–7]. Hence, it is prescribed to analyze dynamic objects using Fourier transform method (FTM). However, single shot based Fourier transform technique also have some drawbacks i.e. spectrum leakage, frequency overlapping, etc. To circumvent these problems, windowed Fourier transform based fringe analysis was proposed in the past [8]. But high processing time of this technique makes it unreliable for real time dynamic applications.

In a fingerprint sensor, the spoof attack can be generated using three different ways: by using an artificial finger made of foreign material, by applying an additional layered structure on the finger, or by using a dead finger. Many efforts have been put in for the detection of fingerprints and undertaking anti-spoofing over the past few decades. Most of these techniques are based on optical coherence tomography (OCT) and its variants [9–13]. Bossen et al. [9] described the identification of internal fingerprint (papillary layer) using frequency domain OCT. Cheng et al. [10] proposed a technique for artificial fingerprint recognition based on OCT and autocorrelation analysis. Artificial fingerprints are constructed using homogeneous material and therefore corresponding correlation co-efficient becomes zero. On the other hand, due to the inhomogeneity beneath the skin of a natural finger, the value of correlation coefficient decreases monotonically with depth. However, the technique is not able to provide security against dead finger spoofing. For that, conventional OCT setup has to be modified using the Doppler effect [11] or a vascular fingerprint has to be captured using swept source OCT [12]. Although, OCT is one of the most promising subsurface imaging methods, it has to produce 3D data even when a single *en face* image is required. This makes OCT slow for imaging and produces unnecessary large data set. Recently, Auksorius et al. [13] proposed a new method called oblique full-field OCT which can produce internal fingerprint image in a single shot without data redundancy. However, OCT-based systems are difficult to align at locations outside the laboratory and have relatively high sensitivity to environmental noise. Also, relatively high cost of tunable laser source and detector increases the overall system cost [14].

Biospeckle analysis is a technique based on scattering phenomenon of light. It has been extensively used as a non-destructive tool to study activities such as ripening, drying, osmosis, Brownian motion, cerebral blood flow, etc. in living objects [15–19]. For analysis of the biospeckle activity two types of methods, visual and numerical, have been explored. Visual methods are preferred over numerical ones because of their ability to generate full-field 2D activity map. Main visual techniques used to obtain information from speckle pattern are Fuji's method, generalized difference (GD), weighted generalized difference, mean windowed difference (MWD), structural function (SF), modified structural function (MSF), etc. [15,20]. Among these, MSF method [20] is based on the summation of the absolute difference between the pixels separated by a certain number of frames. This technique is recent, fast and has been claimed to be accurate in distinguishing between high and low dynamicity of samples.

In this paper, we report our investigation undertaken towards the development of an anti-spoof touchless 3D fingerprint recognition system using single shot fringe projection in conjunction with the biospeckle analysis. The experimental arrangement is very simple and is capable of generating a fringe pattern as well as a speckle pattern. The 3D topographic information of fingerprint is retrieved from a single fringe pattern using FTM based filtering algorithm. Minutiae descriptor based pattern recognition algorithm is implemented to identify the fingerprint of individuals. Biospeckle analysis has been used to distinguish between a real live finger, a fake or a dead one. An algorithm is proposed to capture the dynamicity of a finger surface due to blood flow and muscle reflexes, by improving the MSF, and undertaking the non-normalized histogram based approach to get fast visual and numerical assessment.

2. Basic theory

In optical metrology, fringe projection profilometry plays an important role in measuring three dimensional surface profiles due to their full-field, non-contact, non-destructive, high precision and accurate characteristics. A typical 3D imaging system based on full field sinusoidal fringe projection technique is shown in Fig. 1. Sinusoidal fringe patterns are generated from fringe projecting unit (comprises of an LED and grating) and projected on the test object. Because of the height distribution of the object, fringe modulation takes place and modulated fringe pattern is then captured through an imaging device (CCD Camera) for further processing. On the CCD chip, captured light intensity is a co-sinusoidal function riding on a dc term, which can be mathematically expressed as

$$g(x, y) = a(x, y) + b(x, y)\cos\left[2\pi f_{ox}x + 2\pi f_{oy}y + \Phi(x, y)\right] \quad (1)$$

where, a(x,y) is the average intensity, b(x,y) is intensity modulation, f_{ox} and f_{oy} are carrier frequencies in x and y directions, and Φ(x,y) is the modulated phase information. For extraction of the desired profile information, frequency selective FTM based profile reconstruction algorithm [5] is used. After appropriate Fourier and inverse Fourier transform based filtering operation, desired 3D profile information can be extracted proficiently.

Next, for the detection and recognition of fake fingers, biospeckle analysis is used. When a living object is illuminated by a coherent light

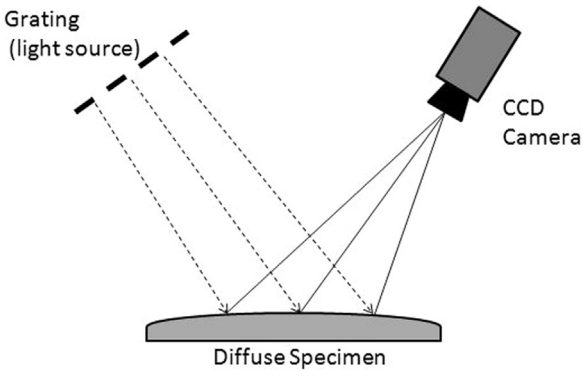

Fig. 1. Basic setup for fringe projection profilometry.

source (e.g. Laser, SLD, etc.), a dynamic interference pattern comprising of a granular structure named as speckle pattern is observed. This technique of generation of activity map of bio specimen is in literature termed as biospeckle. In order to recognize the biological or physical activity of an object, N frames of size $N_x \times N_y$ are captured at a sampling rate f = N/T, where T is the time duration for capturing all the frames. To assess the extent of activity, analysis of spatiotemporal variation of biospeckles is undertaken. Towards this, we improved the visual speckle based MSF approach proposed by Stoykova et al. [20], and combined it with the histogram based non-normalized technique for undertaking the statistics based numerical inspection of visual activity map. Simulation of algorithm includes following steps:

(i) The summation of the absolute difference between pixels separated by 'm' frames, i.e. between images I_k and I_{k+m} is undertaken [20]. A non-negative constant, α, is then multiplied with the MSF to augment the difference in activity between the real and the fake finger without amplifying the unwanted noise, and denoted as MSF*,

$$MSF^*(x, y) = \alpha \times \left(\sum_{k=1}^{N-m} |I_k(x, y) - I_{k+m}(x, y)| \right) \quad (2)$$

where, k is sequence index, x and y are coordinates of intensity matrix I_k, m is the window length and MSF*(x,y) is resulting 2D visual activity map. The value of 'α' should be such that it can shift activity map to a certain extent without compromising the memory compactness of the system.

(ii) To generate a point wise distribution of MSF*(x,y), the calculation of its probability distribution function (PDF) is performed by evaluating its non-normalized histogram map. The region of interest should contain enough number of points to provide a reliable distribution of frequency counts of the estimate values that can be accurately represented through its PDF.

(iii) Quantitative information of the statistical data is extracted from the histogram map by tracing its non-normalized pixel level corresponding to maximum frequency counts. This step provides a numerical characterization of the dynamic speckle activity from 2D visual result.

The difference in activity profile is obtained by repeating Steps (i), (ii) and (iii) for different speckle observations taken with the same sampling frequency at regular intervals or with a different set of samples.

3. Experimental arrangement

Fig. 2 shows schematic of experimental setup for anti-spoof touchless 3D fingerprint profiling using fringe projection and biospeckle analysis. For fingerprint profiling using fringe projection, an LED (dominant wavelength 525 nm, spectral line half width 35 nm) is used in combination with a sinusoidal grating with a period of 0.5 mm. The grating period is selected according to its availability in the laboratory. However, any coarse grating (having range from 0.5 to 10 lines/mm) which does not separate the diffraction orders may be used for projection purpose. For spoof detection using biospeckle analysis, a 15 mW He-Ne laser (wavelength = 632.8 nm) is used as a source of illumination. Laser beam is spatially filtered using a combination of a pinhole of 10 μm diameter and microscopic objective (MO) of magnification of 40X. A precision achromatic doublet lens PAC0888 (Newport Corporation, USA) of focal length 250 mm is used to collimate the spatially filtered beam. Both the LED and laser beams are directed towards the specimen through a beam splitter (BS). As shown in the figure, a finger in the upright position has been chosen as a specimen on which light from both, the LED and the laser, is incident one by one. In order to avoid trembling that can cause a false result, the finger is

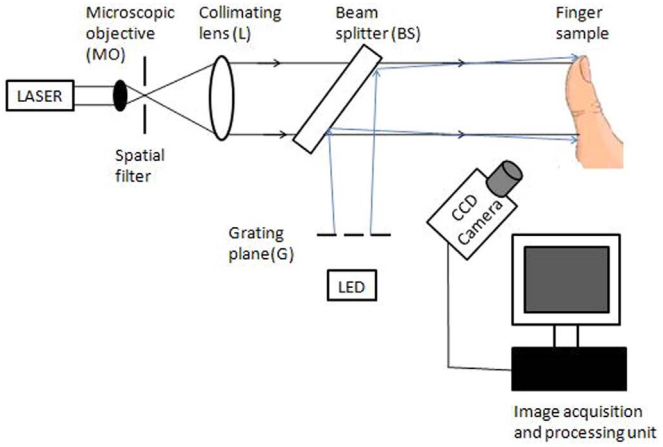

Fig. 2. Schematic of the experimental setup for measurement of anti-spoof touchless 3D fingerprint profile.

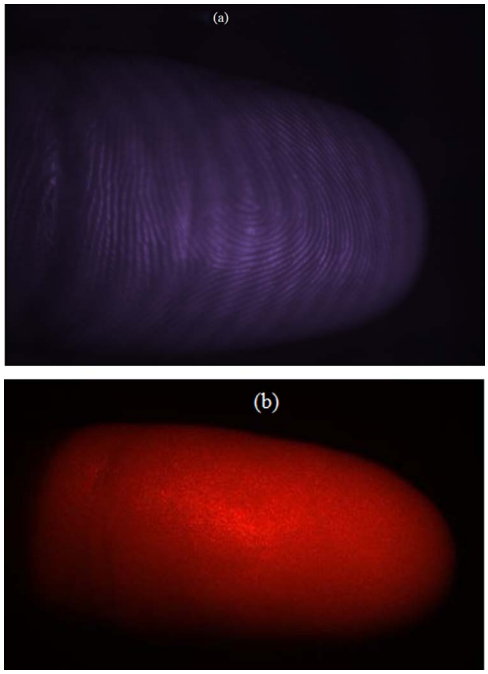

Fig. 3. (a): Deformed fringe pattern of the fingerprint. (b): Speckle pattern of the fingerprint.

placed on a special support during the time data is captured (not shown in the schematic diagram). Following procedure is adapted for recording: First, a fringe pattern generated beyond grating G because of LED illumination is projected onto the sample and the resultant image is recorded using a CCD camera (Basler Corp., frame rate = 32 fps); during this stage the laser remains in the switched off condition. For the generation of 3D fingerprint profile, FTM based filtering algorithm in MATLAB environment is used. In order to avoid reconstruction errors encountered in Fourier based approach, components are placed according to the procedure stated in [21]. Camera calibration was performed using a chessboard having 8 × 8 white and black checkers with each checker size 6 mm x 6 mm. The task applies similar technique as described in [4,22] to calculate basic parameters of CCD camera. In the next step, as the Laser is powered on (and LED switched off), the collimated beam interacts with the rough surface of the finger, resulting in the generation of granular speckle pattern. To study its dynamicity, a series of time-separated speckle patterns were recorded by the CCD camera. Image processing algorithms were developed in MATLAB environment to evaluate biospeckle signature of the finger sample.

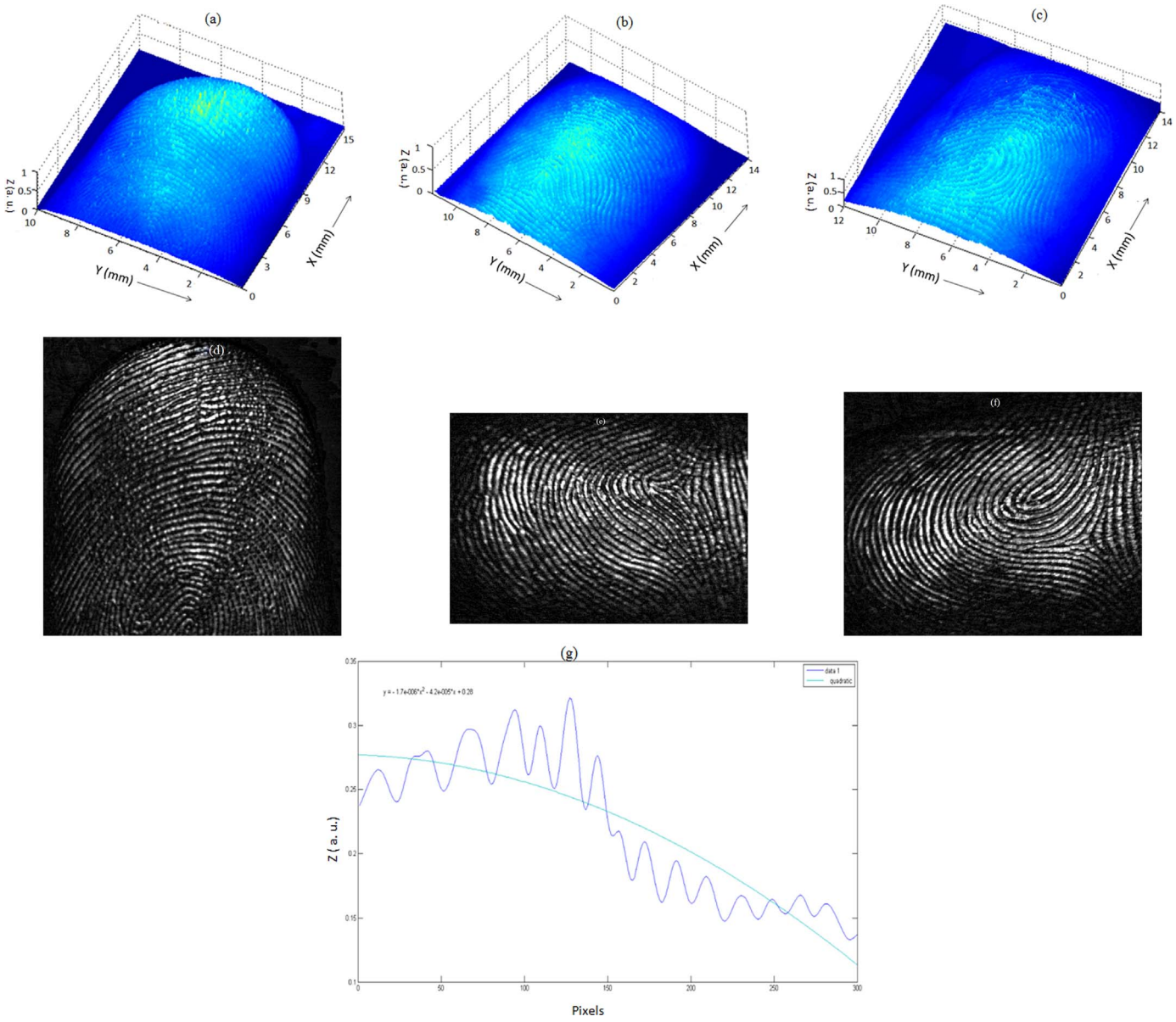

Fig. 4. (a): Reconstructed 3D profile map of sample 1. (b): Reconstructed 3D profile map of sample 2. (c): Reconstructed 3D profile map of sample 3. (d): 2D 'top-hat' filtered profile map of sample 1. (e): 2D 'top-hat' filtered profile map of sample 2. (f): 2D 'top-hat' filtered profile map of sample 3. (g): Ridge-valley pattern.

4. Results and discussion

Results retrieved based on the experimental investigation as discussed in the previous section are shown in Fig. 3. Fig. 3(a) shows the deformed pattern obtained by projecting a sinusoidal fringe using LED source, whereas Fig. 3(b) shows the biospeckle pattern obtained as a result of laser illumination.

As is evident from the Fig. 3(a) the conventional straight line horizontal fringe pattern due to fringe projection is modulated due to the presence of fingertip. The profile information in the resulting pattern is retrieved using frequency selective FTM algorithm implemented in MATLAB environment. Using the proposed 3D sensor, a collection of fingertips were captured and processed to obtain desired 3D information of the fingerprints. The 3D fingerprint has following advantages over 2D imaging:

a) 3D biometrics provides comprehensive information of local space co-ordinate geometry and azimuth. The 2D fingerprint analysis considers each minutia as a triplet {x, y,θ}, where minutiae location co-ordinates are (x, y) and θ is orientation angle. Although, in 3D case a point is represented as {x, y, z, θ, Φ} where (x, y, z) is co-ordinate information and (θ, Φ) are the azimuth which provides it additional two degrees of freedom.
b) 3D biometrics is insensitive to brightness and contrast of illumination source as (x, y, z) of 3D finger can also be represented as (x, y, I(x, y)), where I(x, y) represents the value of gray level of fingerprint image *I* at position (x, y). This also signifies that, the technology is capable of capturing significant information related to fingerprint valleys which can't be achieved using conventional 2D scanners.

Further, in order to obtain the 2D mapping of fingerprints, 'top-hat' filtering and contrast enhancement operations have been undertaken for an ensemble of fingerprints. This 3D and 2D reconstruction is demonstrated for three distinct fingers. Fig. 4(a)-(f) shows the 3D and 2D reconstructed fingerprints for the three selected samples. A small portion of 2D ridge-valley pattern of a finger is plotted against pixel values by applying the line scanning operation to the reconstructed 3D

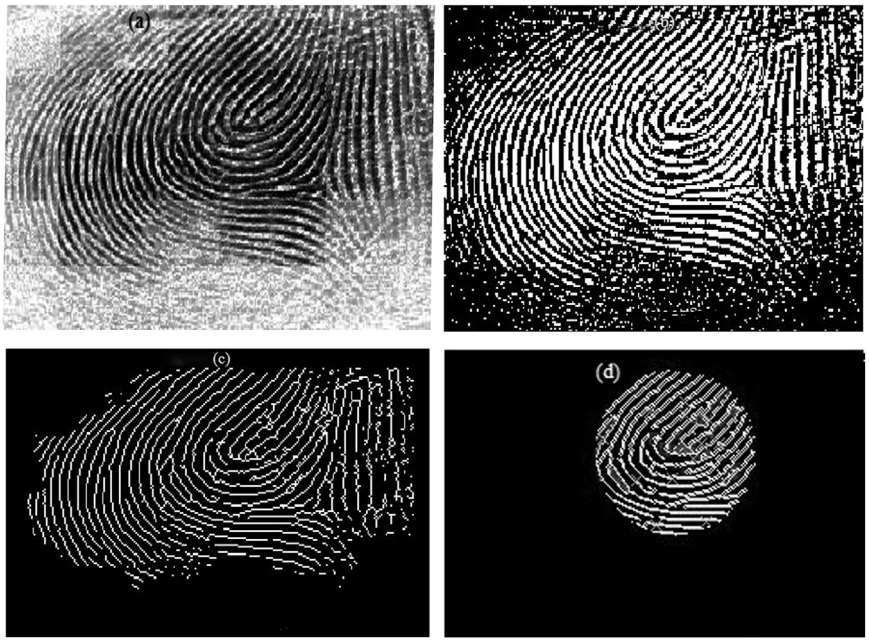

Fig. 5. (a): Enhanced fingerprint by histogram equalization and FFT. (b): Binarized fingerprint. (c): Skeletonised and filtered fingerprint. (d): Feature extraction with corepoint and bounding box.

image (Fig. 4(g)). The average inter-ridge distance is calculated and found to be 20.3 pixels. This is equivalent to 0.452 mm based on the size of CCD pixels. Value of this inter-ridge distance is comparable to the values obtained using a travelling microscope.

For undertaking identification of a fingerprint amongst a set of fingerprints of different persons, minutiae matching based pattern recognition algorithm has been implemented in MATLAB [23,24]. Fingerprint identification process based on minutiae descriptor consists of image enhancement, feature extraction and feature matching. Image enhancement process uses histogram equalization and block wise Fourier filtering (Fig. 5(a)) based image smoothing to enhance the quality of the fingerprint image. Next, binarization (i.e. conversion of grayscale image to '0' and '1' format, Fig. 5(b)) and thinning (i.e. elimination of redundant pixels of ridges till fingerprint ridges are one pixel wide) is performed before extraction of desired features. In order to remove unwanted components from thinned fingerprint, i.e. edge breaks, isolated points, spikes, noise components, etc. are filtered out using morphological operations (Fig. 5(c)). Lastly, different minutiae are marked according to their characteristics. For performing matching between two fingerprints, firstly core point (a point in the direction field where the orientation in the small local neighbourhood around the point have a semi-circular tendency) is detected as this acts as a reference point for fingerprint matching between the test and stored fingerprint. In the next step, a circular bounding box with identical radius is used for both input and reference fingerprints, and respective minutiae are marked (Fig. 5(d)) and counted. Number of different minutiae points in both the samples will be same for the chosen fingerprint. For different fingerprint samples, these numbers vary to a large extent.

To detect genuineness of a finger, three distinct samples i.e. real finger, finger with cello tape (Prime, average thickness = 4 mils), and a false finger made of plastic (Polyvinylchloride mold) [25] are placed one by one in front of the detection system. 100 successive images of 600×600 pixels each are grabbed in the interval of 0.05 s for each sample using the CCD camera. The angle of laser beam was so adjusted to minimize specular reflection and obtain high contrast. 'Quality test protocols' are followed to avoid the generation of false activity map as in [26]. Due to internal blood flow and muscular reflexes, a live finger surface has higher molecular agitation as compared to a layered cello taped finger. This effect is diminished for any finger made of foreign/artificial materials like plastic, silicon, rubber, plaster of paris, etc. Fig. 6 shows the activity map obtained as a result of application of the MSF* function. As indicated by the colorbars, red color represents highest activity and blue represent low activity. Fig. 6(a) which corresponds to the activity map of a real finger, red and yellow colors are dominant representing high dynamicity of the sample. This effect is reduced in the cello taped finger (Fig. 6(b)), and is almost absent in the plastic finger, distinguished clearly by the dominance of the blue color in Fig. 6(c).

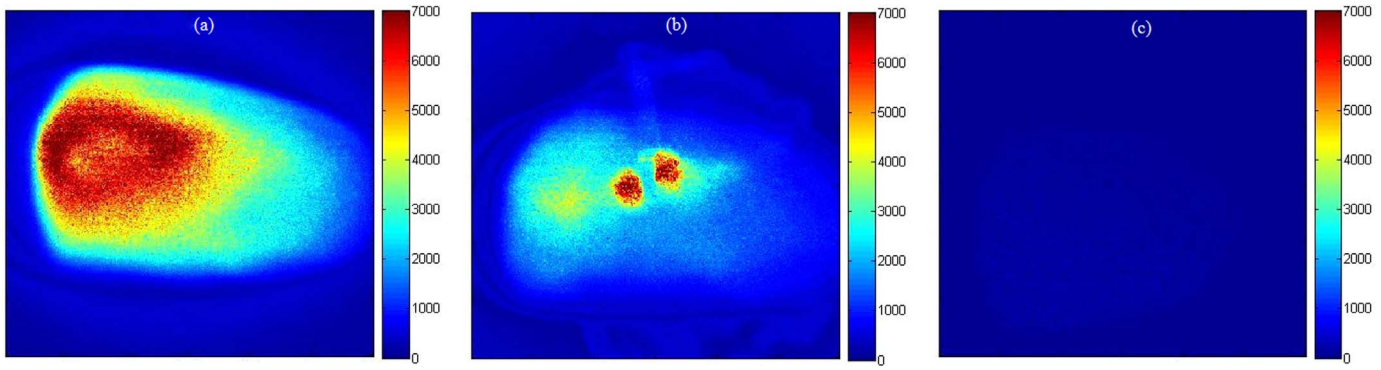

Fig. 6. (a): Activity map of real finger. (b): Activity map of cello taped finger. (c): Activity map of plastic finger.

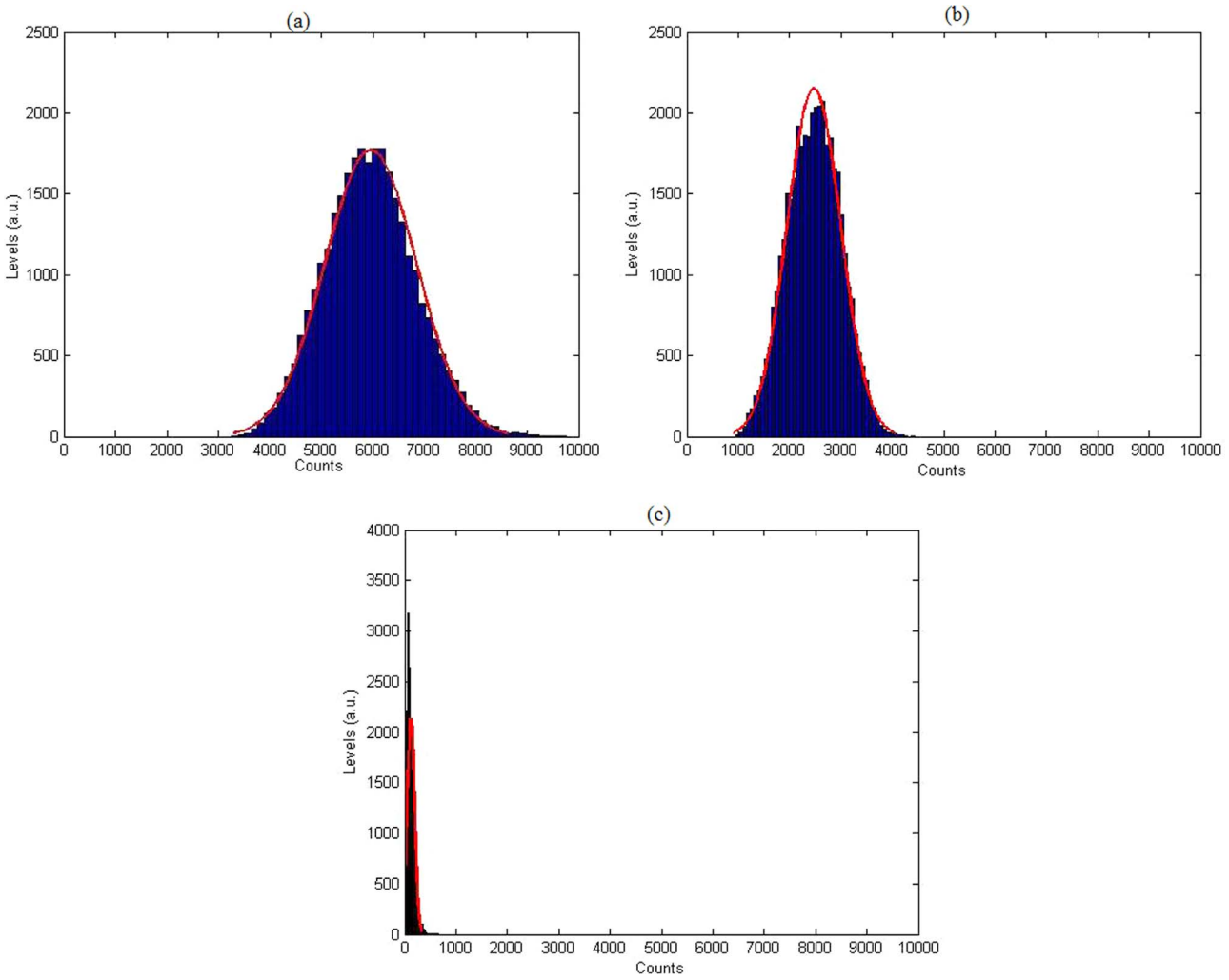

Fig. 7. (a): Histogram map of real finger. (b): Histogram map of cello taped finger. (c): Histogram map of plastic finger.

In the next step, for undertaking the detection of finger spoofing using the numerical analysis, a window of 200×200 pixels for each MSF* image was selected for the investigation, their histogram maps are plotted and the corresponding peaks are traced (Fig. 7). The value of maximum frequency count for the real, cello taped and false finger are obtained to be 5610 (Fig. 7(a)), 2491 (Fig. 7(b)) and 107 (Fig. 7(c)) respectively. These values clearly demonstrate distinction between the real, the layered (cello taped) and the spoofed plastic fingers. The numerical and visual activity map for any dummy finger should be ideally zero since no blood flow exists. However, in practice, a small value exists due to the uncontrolled air flow, temperature fluctuations, internal reflection in optical components and other environmental disturbances.

Trembling (or tremor), a rhythmic vibration generated due to muscular contraction of animal body, plays a vital role on liveliness measurement in the proposed sensor. Over the years, many researchers devoted efforts to understand tremor frequency, displacement and acceleration behaviour. In this route, Schafer et al. [27] calculated the finger tremor rate to be 10 cycles/second. Halliday et al. [28] reported that the displacement of fingerprint is insignificant above the frequency of 12 cycle/second and also shown through experimental investigation that with added support (or weight) in the finger (as also done in this set up) the tremor frequency drops to the order of (1/3)rd of natural frequency. In the proposed set up, we have used a CCD Camera with a frame rate that is considerably higher than highest possible trembling frequency in order to nullify its effect in 3D shape measurement. As soon as an individual die, the functioning of heart and lungs stops and tremor frequency decreases considerably. When heart stops functioning, the red blood cells (RBC), being heavier, sink through the serum due to gravitational force. This is known as Livor mortis. It starts within 20–30 min after the death and becomes visible within 2 h. On the other hand, when a person stops breathing, the metabolic production of adenosine triphosphate (ATP) in the cells stops immediately. ATP is a chemical that is required for relaxation of muscle fibers after its contraction. As a result of ATP depletion in the body, muscle fibers lock-up and stiffen (as a result tremor frequency becomes zero). This is known as Rigor mortis [29]. It's settling time is almost the same as that of Livor mortis. Due to these two phenomena, biospeckle activity of a dead finger is the same as that of an artificial finger. Hence, this method is robust against dead finger spoofing too.

5. Conclusions

In the present study, we have successfully demonstrated a real-time setup for anti-spoof touchless 3D fingerprint recognition. Highlights of the proposed setup include its low cost, extreme simplicity, the requirement of fewer components, simple algorithms and its ability to be commercialized. Following points can be retrieved from this experimental investigation:

i) We observed that, the fingerprint profiling is successfully undertaken using single shot fringe projection. Lack of environmental noise, alleviation of compensation optics, applicability on diffuse surface, etc. makes it a better alternative than interferometry,

tomography and deflectometry.

ii) The 3D shape reconstruction of grabbed fingerprint is performed using frequency selective FTM based shape reconstruction algorithm. This method is better than other fringe analysis techniques (e.g. Phase shifting technique) because of fast processing with the only single fringe pattern, non-mechanical scanning, etc. Although replicating 2D fingerprint is an easy task, it is almost impossible to replicate a 3D fingerprint.

iii) For spoof detection, biospeckle signature due to blood flow in the finger is utilized. A combination of MSF* and non-normalized histogram techniques is used for visual and numerical inspection. With use of this technique distinction between a real finger, false finger and dead finger can be performed efficiently.

iv) Overall the proposed technique is very simple, fast, low cost and full field.

Further investigations are underway to develop a foolproof 3D fingerprint matching process/algorithm which will add one more degree of security to the fingerprint detection system. In future, the components used in the proposed technique can be miniaturized and fabricated in a single unit to make a commercial anti-theft fingerprint scanner which is capable of detecting and matching the type of spoofing along with a 3D profile of the fingerprint.

Acknowledgement

This work is supported by Department of Electronics and Information Technology (DeitY), India, and Science and Engineering Research Board (SERB), Department of Science and Technology with file number EMR/2016/003115. The authors are grateful to the anonymous reviewers for several constructive suggestions that have helped increase the quality of the work presented.

References

[1] Hawthorne M. Fingerprints: analysis and understanding. CRC Press: Taylor & Francis group; 2009.
[2] Parziale G, Diaz-Santana E, Haukae R. A multi-camera touchless device to acquire 3D rolled-equivalent fingerprints. Int Conf Biom 2006:224–50.
[3] Wang YC, Hassebrook LG, Lau DL. Data acquisition and processing of 3-D fingerprints. IEEE Trans Inf Forens Sec 2010:1–9.
[4] Huang S, Zhang Z, Zhao Y, Dai J, Chen Y, Xu Y, Zhang E, Xie L. 3D fingerprint imaging system based on full-field fringe projection profilometry. Opt Lasers Engg 2014;52:123–30.
[5] Gorthi SS, Rastogi P. Fringe projection techniques: whither we are? Opt Lasers Engg 2010;48:133–40.
[6] Su X, Zhang Q. Dynamic 3D shape measurement method: a review. Opt Lasers Engg 2010;48:191–204.
[7] Rajsekhar G, Rastogi P. Fringe analysis: Premise and perspective. Opt Lasers Engg 2012;50. [iii-x].
[8] Kemao Q. Application of windowed Fourier fringe analysis in optical measurement: a review. Opt Lasers Engg 2015;66:67–73.
[9] Bossen A, Lehmann R, Meier C. Internal fingerprint identification with optical coherence tomography. IEEE Phot Technol Lett 2010;22:507–9.
[10] Cheng Y, Larin KV. Artificial fingerprint recognition by using optical coherence tomography with autocorrelation analysis. Appl Opt 2006;45:9238–45.
[11] Rollins AM, Yazdanfar S, Barton JK, Izatt JA. Real-time in vivo color Doppler optical coherence tomography. Journ Biomed Opt 2002;7:123–9.
[12] Liu G, Chen Z. Capturing the vital vascular fingerprint with optical coherence tomography. Appl Opt 2013;52:5473–7.
[13] Auksoriusand E, Boccara AC. Fingerprint imaging from the inside of a finger with full-field optical coherence tomography. Biomed Opt Exp 2015;6:4465–71.
[14] Dhanotia J, Prakash S, Bhatia V, Prakash S. Fingerprint detection and mapping using phase shifted coherent gradient sensing technique. Appl Opt 2016;55:5316–21.
[15] Zdunek A, Adamiak A, Piecywek PM, Kurenda A. The biospeckle method for the investigation of agricultural crops: a review. Opt Lasers Engg 2014;52:276–85.
[16] Pajuelo M, Baldwin G, Rabal HJ, Cap N, Arizaga R, Trivi M. Bio-speckle assessment on bruising in fruits. Opt Lasers Engg 2003;40:13–24.
[17] Jayanthy AK, Sujatha N, Reddy MR. Non-invasive assessment of static scatterer concentration in phantom body fluids using laser speckle contrast analysis technique. Opt Lasers Engg 2011;49:553–6.
[18] Godinho RP, Silva MM, Nozela JR, Braga RA. Online biospeckle assessment without loss of definition and resolution by motion history image. Opt Lasers Eng 2012;50:366–72.
[19] Tripathy MM, Hajjarian Z, Cott EMV, Nadkarni SK. Assessing blood coagulation status with laser speckle rheology. Biomed Opt Exp 2014;5:817–31.
[20] Stoykova E, Nazarova D, Berberova N, Gotchev A. Performance of intensity-based non-normalized pointwise algorithms in dynamic speckle analysis. Opt Exp 2015;23:25128–42.
[21] Su X, Chen W. Fourier transform profilometry: a review. Opt Lasers Engg 2001;35:263–4.
[22] Labati RD, Genoves A, Piuri V, Scotti F. Towards unconstrained fingerprint recognition: a fully touchless 3-D system based on two view on the move. IEEE Trans Sys Man Cyb Sys 2015;46:01–18.
[23] Hong L, Wan Y, Jain A. Fingerprint image enhancement: algorithm and performance evaluation. IEEE Trans Pattern Anal 2002;20:777–89.
[24] Jie Y, Yi fang Y, Renjie Z, Qifa S. Fingerprint minutiae matching algorithm for real time system. Pattern Rec 2006;39:143–6.
[25] Menning G, Stoeckhert K. Mold-making handbook: for the plastic engineer. 2nd ed Hancer Gard Pub; 1998.
[26] Moreira J, Cardoso RR, Braga RA. Quality test protocol to dynamic laser speckle analysis. Opt Lasers Engg 2014;61:8–13.
[27] Schafer EA. On the rhythm of muscular response to volitional impulses in man. J Physiol 1886;7:111–7.
[28] Halliday AM. An analysis of the frequencies of finger tremor in healthy subjects. J Physiol 1956;134:600–11.
[29] Dolinak D, Matshes EW, Lew EO. Forensic pathology: principles and practice. Elsevier academic press; 2006.

Mr. Amit Chatterjee was born in 1992 in India. He obtained his Bachelor's degree in Electronics and Communication Engineering, from Asansol Engineering College, under West Bengal University of Technology, in 2014 and Master degree in Digital Instrumentation from Devi Ahilya University, Indore in 2016. He is pursuing Doctor of Philosophy (Ph.D.) degree in Electrical Engineering Department from Indian Institute of Technology-Indore, Indore (M.P.), India. His area of interest is Optical Instrumentation, Automated Interferogram Processing and Biospeckle Analysis.

Dr. Vimal Bhatia received Ph.D. from Institute for Digital Communications at The University of Edinburgh, UK in 2005. He is currently working as Associate Professor with IIT Indore. His research interests are in the algorithms and product development for future communication, signal processing and optical systems. He currently has 85 publications and filed 10 patents. He is Senior Member IEEE and reviewer for OSA, IEEE, Elsevier and Springer.

Dr. Shashi Prakash is Professor at Department of Electronics & Instrumentation, Institute of Engineering - & Technology, Devi Ahilya University, Indore, India. He joined Devi Ahilya University as Lecturer in 1992 and was promoted to the post of Reader in 2002. He did his M. Tech and Ph.D. both from Indian Institute of Technology, Delhi, New Delhi in 1992 and 2003, respectively. Between 1998 and 2000, he was CSIR-Research Associate, working at Indian Institute of Technology, Delhi, New Delhi. In 2009, he had a stint as 'Visiting Foreign Researcher' in Department. of Electrical & Electronics Engineering, Niigata University, Niigata, Japan. His research interests are in the area of Optical Metrology/Communication, and has published more than 85 research papers in International Conferences and Journals.